Article

Journal of
Nanoscience and Nanotechnology
Vol. 19, 492–497, 2019
www.aspbs.com/jnn

Preparing SnO_2/MWCNT Nanocomposite Catalysts via High Energy Ball Milling

Krisztian Nemeth[1], Zoltan Pallai[1], Balazs Reti[1], Peter Berki[1], Zoltan Nemeth[1,2], and Klara Hernadi[1,*]

[1] *Department of Applied and Environmental Chemistry, University of Szeged, Rerrich tér 1, Szeged H-6720, Hungary*
[2] *Institute of Chemistry, University of Miskolc, Miskolc-Egyetemváros, Miskolc, H-3515, Hungary*

Ball milling method was used to fabricate successfully tin dioxide (SnO_2)/multi-walled carbon nanotubes nanocomposite materials using $SnCl_2 \times 2H_2O$ as precursor together with soda and salt as admixture. The as-prepared materials were characterized by transmission electron microscopy, scanning electron microscopy with energy-dispersive X-ray spectroscopy, Raman microscopy, and X-ray diffraction techniques. Observations revealed that applying both soda and salt are advantageous for increasing dispersity of tin dioxide nanoparticles on the surface of carbon nanotubes. These multi-walled carbon nanotube-based composites are promising candidates as thick film gas sensors or catalysts. Results indicate that SnO_2/MWCNT composites can be achieved under solvent free dry conditions, too.

Keywords: Carbon Nanotubes, Tin Dioxide, Dry Ball Milling, Nanocomposite.

1. INTRODUCTION

Due to their excellent physical, mechanical, and unique electronic properties, carbon nanotubes (CNTs) have affected research community since their discovery.[1] CNTs are considered as capable contestants for many applications such as composite materials,[2] field emission materials[3] or chemical sensors.[4,5] Combining CNTs with various nanoparticles can result in exceptional performances in solar cells, catalysts or nanoelectronic devices.[6–9] Due to their high theoretical electrical conductivity, high aspect ratio and good mechanical properties, carbon nanotubes can offer the necessary electronic matrix for anode materials.[10]

From recent investigations, it can be learned that the attachment of various inorganic compounds such as SnO_2 onto single-walled (SWCNTs) or multi-walled carbon nanotubes (MWCNTs)[4,11–14] can be achieved via different synthesis methods. MWCNTs were decorated with SnO_2 by the chemical solution method in which acid-treated MWCNTs was used.[15] Zhu et al.[16] reported the preparation of MWCNT/SnO_2 core–shell structures by a double coating process in a wet chemical route. Du et al. synthesized SnO_2 nanotubes on CNTs by a layer-by-layer technique.[17] In some preliminary experiments, it has been observed that SnO_2 nanoparticles could be deposited onto the surface of MWCNTs to form a uniform layer by CVD technique.[12]

As one of the most important semiconductor oxide, SnO_2 has been studied using for different purposes such as photocatalysts,[18,19] lithium ion batteries[20] or sensors.[21] On the other hand, MWCNT could be considered as a good electron acceptor because of its unique structure.[22] Beyond potential photocatalytic efficiency,[23] several papers were already published about special sensing applications. For the efficient detection of SO_2 gas, MWCNT-SnO_2 and RGO-SnO_2 hybrid nanocomposite sensors were prepared by incorporating MWCNTs and RGO (reduced graphite oxide) into SnO_2 nanoparticle colloidal solution respectively by chemical route.[24] Pal et al.[25] achieved high sensitivity, stability, ultrafast response toward sub-ppm acetone detection with a good resolution (i.e., promising material for diabetes sensor) just by using MWCNTs as a substrate for nanocrystalline SnO_2 prepared through a facile sol–gel technique. In our previous investigations, we successfully fabricated SnO_2/MWCNT nanocomposite by the sol–gel method and their gas sensing properties were also studied.[26,27]

In order to exploit good electricity of MWCNT and semiconductor properties of SnO_2, the aim of current work was to develop controllable synthesis method for SnO_2/MWCNT composites. Since our former results

*Author to whom correspondence should be addressed.

 1533-4880/2019/19/492/006 doi:10.1166/jnn.2019.15774

proved[28] that using either impregnation or hydrothermal synthesis the morphology of composite is strongly influenced by the applied solvents. Thus, in order to investigate the previously mentioned parameters, we applied solvent free method via planetary ball milling. The morphology of the final product was investigated: beside vulnerability of MWCNT under milling conditions, the effect of "inert" compounds on the structure of the final product was also studied.

2. EXPERIMENTAL DETAILS

MWCNT was prepared from acetylene (CVD method) in a rotary oven at 720 °C using Fe, $Co/CaCO_3$ catalyst.[29] This synthesis method using $CaCO_3$ catalyst enables a highly efficient selective growth of MWCNT having a clean surface, free of any amorphous carbon or carbonaceous particles, thus suitable for effective bonding between MWCNT and precursors (see Fig. 1). High graphitization also prevents pristine MWCNT from fragmentation under mechanical stress during ball milling.

Fritsch Pulverisette 6 type planetary ball mill, equipped with a 250-mL grinding bowl and 10 WC balls of 10 mm size were used for homogenization. The rotational speed was 400 rpm. In order to avoid damage of MWCNT, the treatment time of planetary ball milling was set to a low value, namely 60 minutes.

In the first series, $SnCl_2$ ($SnCl_2 \times 2H_2O$ from Molar Chemical) was added as precursor together with MWCNT for the preparation of composites, using a mass ratio of 8:1. To form SnO_2 directly during ball milling,[30] Na_2CO_3 (soda, Reanal) was also added to the system in the second series (the presence of soda is denoted in superscript before the name of the composite):

$$SnCl_2 + Na_2CO_3 \rightarrow SnO + 2NaCl + CO_2$$

To avoid aggregation of forming SnO_2 nanoparticles, in the third series NaCl (salt, Spektrum-3D) was also placed into the bowl before milling (the presence of salt is denoted in subscript before the name of the composite). For better comparison of SnO_2 nanoparticles, each sample was prepared without carbon nanotubes, too. The formed and/or added NaCl was washed off with distilled water from the system after milling.

The following components were mixed in the bowl:

$SnCl_2$ (with or without MWCNT):Na_2CO_3:

NaCl in 1:1:1 molar ratio

and the samples were denoted as follows:

$$^{\text{soda}}_{\text{salt}}SnO_2/\text{MWCNT}$$

Samples were heat treated in air at 450 °C for 3 hours.

Under the most promising conditions, the SnO_2/MWCNT mass ratio was reduced to 4:1 and 2:1 hoping that the portion of segregated SnO_2 can be controlled in this way.

In order to verify the formation of any decoration on the surface of MWCNTs, the resulted powders were investigated with transmission electron microscopy (Philips CM 10, FEI Technai G^2 20 X-TWIN (TEM)). A small amount of sample was sonicated in ethanol. A few drops of this suspension were dribbled onto the surface of the copper grid. Scanning electron microscopy (Hitachi S-4700 Type II (SEM)) with a Röntec XFlash Detector 3001 SDD device was used to identify tin oxide nanoparticles. The crystalline structure of the inorganic layer was also studied by powder X-ray diffraction—XRD—(Rigaku Miniflex II Diffractometer) method using Cu Kα radiation. Raman spectroscopy measurement was done on a Thermo Scientific DXR Raman microscope with a 532 nm laser (5 mW).

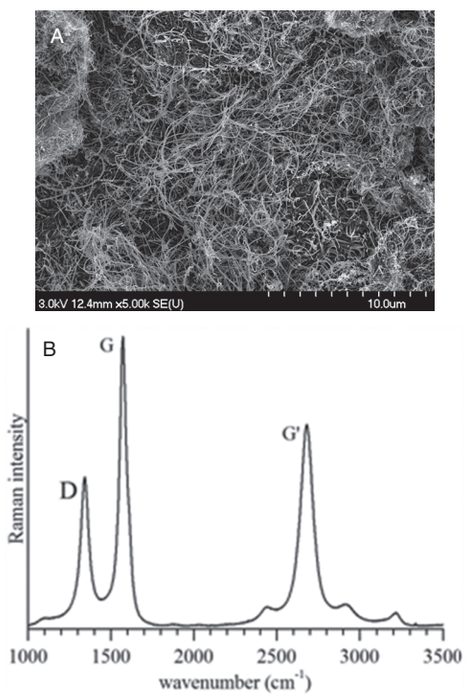

Figure 1. SEM micrograph (A) and Raman spectrum (B) of pristine MWCNTs.

3. RESULTS AND DISCUSSION

3.1. X-ray Diffraction Characterization

To ascertain the crystallinity, all samples were characterized by XRD technique. However, because of significant similarities, only one diffraction pattern is presented in the current study. On the X-ray diffraction patters the characteristic diffractions of SnO_2 can be identified, namely, $2\theta = 26.5°$—(110), 33.8°—(101), 37.9°—(200), 51.8°—(211), and 54.6°—(220). Approximately at $2\theta = 25°$ a shoulder can be seen which is most presumably the characteristic reflection of MWTNs. Since crystal plane (002)

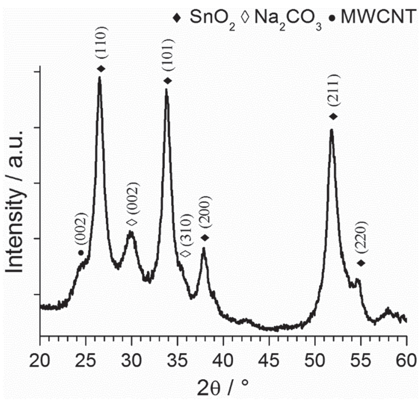

Figure 2. X-ray diffractogram of ${}^{soda}SnO_2$/MWCNT nanocomposite after ball milling of $SnCl_2$, Na_2CO_3 and MWCNT.

of multi-walled carbon nanotubes and reflection (110) of SnO_2 overlap, their identification is ambiguous by means of X-ray diffraction. The distinctive X-ray diffraction pattern of NaCl is not detectable; thus, only traces of this material can be present in the samples. Hence, X-ray diffraction results confirmed that crystalline SnO_2 can be obtained via ball milling of $SnCl_2$ precursor. Figure 2 illustrates characteristic reflections of ${}^{soda}SnO_2$/MWCNT nanocomposite obtained after ball milling of $SnCl_2$, Na_2CO_3 and MWCNT together. In addition to the above mentioned diffraction peaks, a broad reflection appears at around $2\theta = 30°$ and a noticeable shoulder at around $2\theta = 35°$. These features can be attributed to the presence of Na_2CO_3.

3.2. Raman Microscopy Measurements

In order to resolve former uncertainties, Raman microscopy measurements were also implemented. From Raman spectra in Figure 3 conclusions can be drawn referring to the nature of both constituents and final nanocomposites. Regarding multi-walled carbon nanotubes, Raman spectra verified their good quality of high degree of graphitization. From D, G and G′ peaks (see Table I)

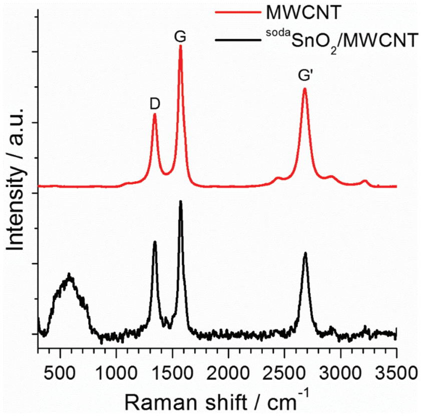

Figure 3. Raman spectra of pristine MWCNT and ${}^{soda}SnO_2$/MWCNT nanocomposite after ball milling of $SnCl_2$, Na_2CO_3 and MWCNT.

Table I. Raman intensity ratios of pristine MWCNT and SnO_2/MWCNT.

	MWCNT	SnO_2/MWCNT
I_D/I_G	0.51	0.69
$I_{G'}/I_G$	0.70	0.58
$I_{G'}/I_D$	1.35	0.84

well-graphitized structure of pristine MWCNT is proved, moreover, change in intensity ratios of SnO_2/MWCNT nanocomposite suggests a minor change in the structure of MWCNT which can be correlated with the forming chemical bond between constituents. The possibility that this minor change is coming from the damage caused by ball milling can be excluded by our former results.[31] Since there is a broad peak in the region of 400 cm^{-1} and 800 cm^{-1}, identification of SnO_2 from Raman spectra is unfortunately doubtful. Characteristic peak of SnO_2 could be expected at around 630 cm^{-1} but it is probably covered by the sign of semi-crystalline $SnO(OH)_2$. However, this observation is in accordance with X-ray diffraction results described above.

3.3. Energy Dispersive X-ray Analysis

In order to characterize the quality of nanoparticles in as-prepared samples, energy dispersive X-ray analysis (EDX) was performed in the SEM instrument for each nanocomposite. Since EDX spectra showed significant similarity, only one EDX spectrum is presented here (Fig. 4). The most important signals originate from carbon (C) oxygen (O) and tin (Sn), respectively, which proves the constituents of nanocomposites. It is worthy notified that no sodium peak was detectable, thus removal of NaCl from the sample was successful.

3.4. Transmission Electron Microscopy Investigations

Transmission electron microscopy revealed that materials, obtained without admixture, e.g., ball milling of tin chloride precursor and MWCNT, possess non-uniform morphology. Figure 5 shows TEM micrographs for SnO_2 crystals after ball milling of $SnCl_2$ (A) and SnO_2/MWCNT nanocomposite after ball milling of $SnCl_2$ and MWCNT (B), respectively. In Figure 5(A) both small

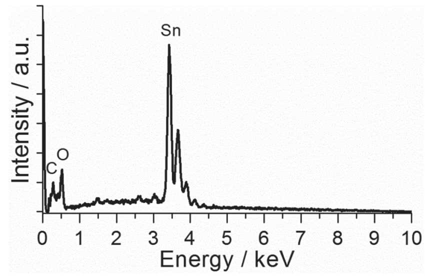

Figure 4. Representative EDX analysis of ${}^{soda}SnO_2$/MWCNT nanocomposite after ball milling of $SnCl_2$, Na_2CO_3 and MWCNT.

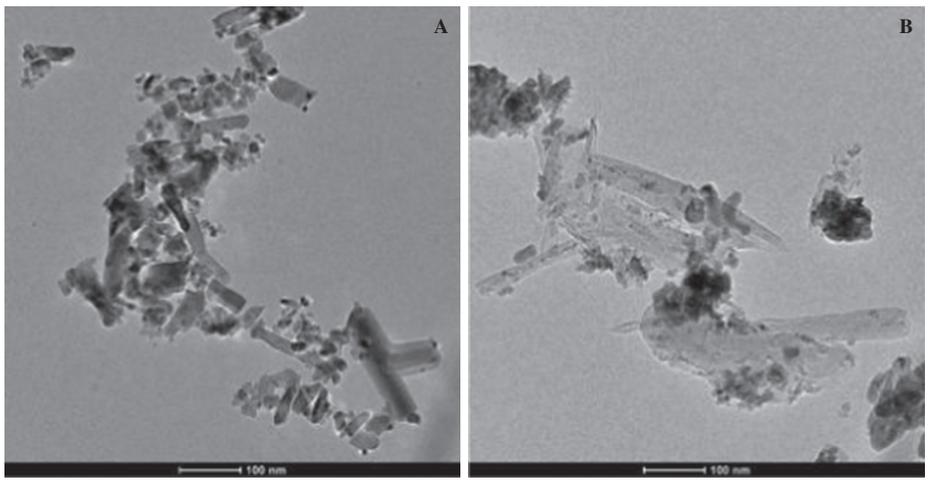

Figure 5. TEM images of SnO_2 crystals after ball milling of $SnCl_2$ (A) and SnO_2/MWCNT nanocomposite after ball milling of $SnCl_2$ and MWCNT (B).

crystals and nanorods can be observed. Shearing stress during high energy ball milling might affect the shape of forming SnO_2 crystals; therefore we applied simple heat treatment and made sure of the formation of nanorods via annealing. This is in accordance with former investigations,[32] which resulted in SnO(2) nanowires and nanorods were one dimensional (1D) structures with widths and lengths of 50–200 nm and several micrometers, respectively. From the analysis of TEM images of nanocomposites (Fig. 5(B)), it can be stated that MWCNT is strongly damaged, fragmented, and forming SnO_2 nanoparticles are not deposited onto its surface rather form segregated clusters. We suppose that without admixture $SnCl_2$ precursor can form very reactive chlorine-containing species during ball milling which react with MWCNT (the only reaction partner in the present instance) in the milling bowl. Due to significant fragmentation and low SnO_2 coverage observed, further experiments were carried out under modified conditions.

The presence of admixture, e.g., can hinder undesirable effects, as chemical reaction between $SnCl_2$ and Na_2CO_3 result in less reactive by-products such as NaCl and CO_2. Accordingly, the following samples were prepared with three constituents. From TEM image of $^{soda}SnO_2$ crystals in Figure 6(A) it can be seen that nano-sized SnO_2 particles form bigger aggregates, however, nanorods cannot be observed any more. TEM investigations also revealed that in $^{soda}SnO_2$/MWCNT nanocomposite there are undamaged multi-walled carbon nanotubes (with no fragmentation and unvarying aspect ratio) densely covered by SnO_2 nanoparticles (Fig. 6(B)). Nevertheless, beside $^{soda}SnO_2$/MWCNT nanocomposite significant amount of separated SnO_2 aggregates like the one described in Figure 6(A) was detected. These bigger particles can

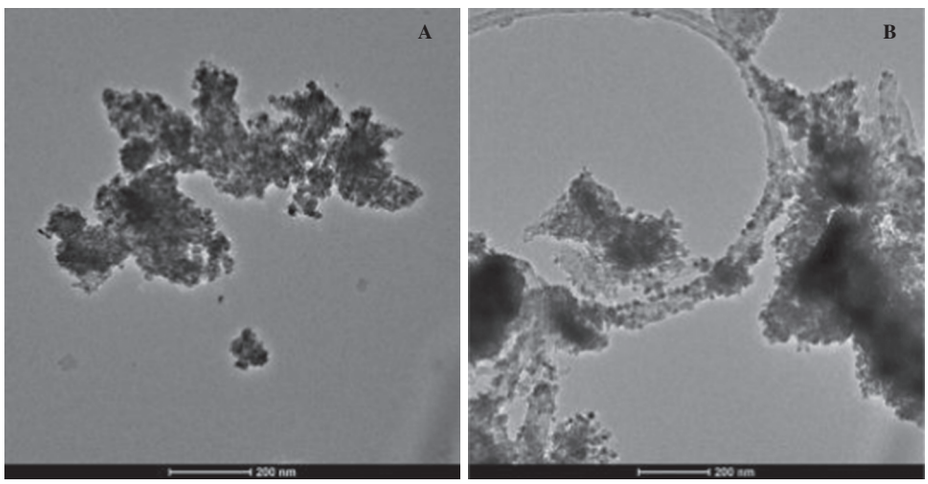

Figure 6. TEM images of $^{soda}SnO_2$ crystals after ball milling of $SnCl_2$ and Na_2CO_3 (A) and $^{soda}SnO_2$/MWCNT nanocomposite after ball milling of $SnCl_2$, MWCNT and Na_2CO_3 (B).

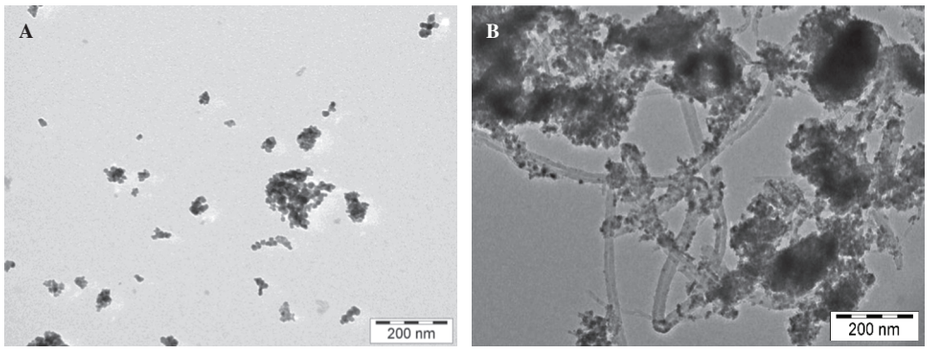

Figure 7. TEM images of $^{soda}{}_{salt}SnO_2$ crystals after ball milling of $SnCl_2$, Na_2CO_3 and NaCl (A) and $^{soda}{}_{salt}SnO_2$/MWCNT nanocomposite after ball milling of $SnCl_2$, MWCNT, Na_2CO_3 and NaCl (B).

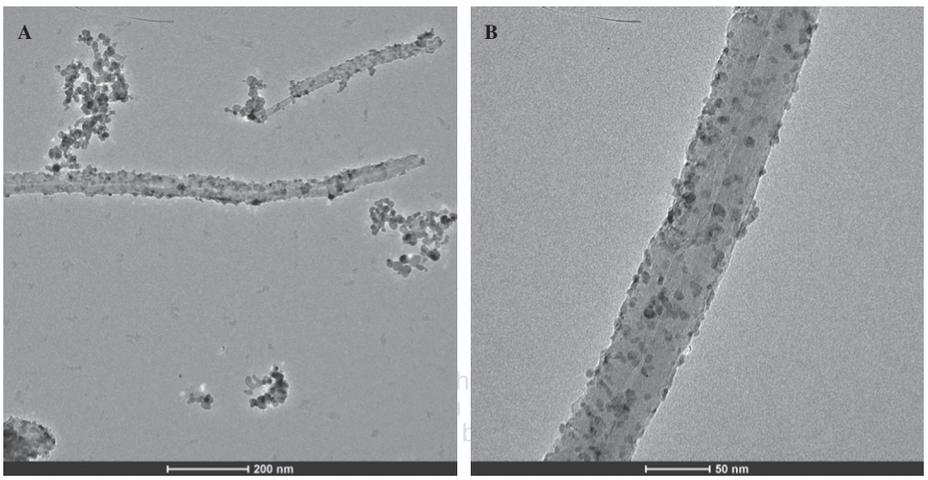

Figure 8. TEM images of $^{soda}SnO_2$/MWCNT nanocomposite prepared with 4:1 (A) and 2:1 (B) mass ratio.

even enshroud desired nanocomposites. This experience inspired us to further modify experimental conditions.

In the hope of avoiding the formation of segregated particles, another admixture (e.g., inert NaCl) was added to the system. In the case of $^{soda}{}_{salt}SnO_2$ crystals it can be concluded from TEM observations (Fig. 7(A)) that aggregation was successfully suppressed. In the case of $^{soda}{}_{salt}SnO_2$/MWCNT nanocomposite (see Fig. 7(B)) multi-walled carbon nanotubes decorated with SnO_2 nanoparticles formed again, however, the amount of separated SnO_2 phases was not reduced significantly.

From TEM analysis it can be concluded that both $^{soda}SnO_2$/MWCNT and $^{soda}{}_{salt}SnO_2$/MWCNT nanocomposites contained the desired ensemble thus they are worthy for further experiments.

3.5. Tuning Mass Ratio of SnO_2 and MWCNT

In order to reduce the amount of segregated SnO_2 particles, synthesis conditions were modified as follows: SnO_2:MWCNT mass ratio was reduced to 4:1 and 2:1, respectively, and ball milling was carried out in the presence of Na_2CO_3 admixture. TEM images in Figures 8(A) and (B) illustrates well that using mass ratio of 4:1 $^{soda}SnO_2$/MWCNT nanocomposite is still accompanied together by separated SnO_2 particles, however, their amount is already significantly lowered. On the other hand, with the mass ratio of 2:1 (Fig. 8(B)) the separation of SnO_2 nanoparticles is completely inhibited. Summing up of our observations it can be stated that choosing proper mass ratio of SnO_2:MWCNT, high energy ball milling is a suitable method for the fabrication of SnO_2/MWCNT nanocomposite. With lower mass ratio further benefit can be gained: former investigations revealed that for (photo)catalytic purposes a non-homogeneous coverage is advantageous.[33]

4. CONCLUSION

The aim of this work was to produce SnO_2/MWCNT nanocomposite under solvent free conditions via high energy ball milling for homogenization. $SnCl_2$ and MWCNT were used as starting materials—with or without admixture(s)—under different synthesis conditions. Physico-chemical characterization revealed that the addition of admixture(s) and the MWCNT content of the

synthesis mixture significantly affected the morphology of final products. While the crystal structure was rather independent of the nature of initial compounds (from the results of XRD diffraction, Raman microscopy and energy-dispersive X-ray spectroscopy), transmission electron microscopy analysis confirmed that components have a strong influence on the morphological feature of the nanocomposite. Without admixtures, the structure of multiwalled carbon nanotubes severely damaged, probably due to the formation of aggressive chemicals from the tin precursor. Applying soda or soda and salt together prevented MWCNT from significant fragmentation, thus proved to be suitable methods for SnO_2/MWCNT nanocomposite synthesis. NaCl, either formed or added, can be easily and successfully removed from the product; however, to reduce the amount of segregated SnO_2 particles only $^{soda}SnO_2$/MWCNT nanocomposites were prepared with different mass ratios. Using SnO_2:MWCNT mass ratio of 2:1 resulted in "clean" SnO_2/MWCNT nanocomposite without segregated inorganic particles. It was proved that unbeneficial effect of various solvents can be avoided by another synthesis technique. Changing admixtures and mass ratios during high energy ball milling, both the morphology and the composition of the final product can be controlled. Furthermore, these shape tailored materials are rather promising for future application in many fields such as effective (photo)catalysis or special sensing.

Acknowledgment: Special thanks to Professor László Forró and his research group in École Polytechnique Fédérale de Lausanne (EPFL) to provide us the multiwalled carbon nanotubes. This work was supported by grants from Switzerland through Swiss Contribution (SH/7/2/20). Klara Hernadi is very grateful for the financial support provided by the GINOP-2.3.2-15-2016-00013 project. Krisztian Nemeth thanks to Országos Tudományos Kutatási Alapprogramok (OTKA NN114463) to financial support. Zoltan Nemeth is thankful for the financial support for the European Union and the Hungarian Government in the framework of the GINOP 2.3.4-15-2016-00004 "Advanced materials and intelligent technologies to promote the cooperation between the higher education and industry."

References and Notes

1. S. Iijima, *Nature* 354, 56 (**1991**).
2. H. B. Chu, L. Wei, R. L. Cui, J. Y. Wang, and Y. Li, *Coord. Chem. Rev.* 254, 1117 (**2010**).
3. S. Frank, P. Poncharal, Z. L. Wang, and W. A. de Heer, *Science* 280, 1744 (**1998**).
4. Y. L. Liu, H. F. Yang, Y. Yang, Z. M. Liu, G. L. Shen, and R. Q. Yu, *Thin Solid Films* 497, 355 (**2006**).
5. M. T. Humayun, R. Divan, Y. Z. Liu, L. Gundel, P. A. Solomon, and I. Paprotny, *J. Vac. Sci. Technol. A* 34, 7 (**2016**).
6. H. Y. Dong and K. Lu, *Int. J. Appl. Ceram. Technol.* 6, 216 (**2009**).
7. P. Diao and Z. F. Liu, *J. Phys. Chem. B* 109, 20906 (**2005**).
8. G. H. Jiang, X. Y. Zheng, Y. Wang, T. W. Li, and X. K. Sun, *Powder Technol.* 207, 465 (**2011**).
9. D. R. Kauffman, Y. F. Tang, P. D. Kichambare, J. F. Jackovitz, and A. Star, *Energy Fuels* 24, 1877 (**2010**).
10. B. J. Landi, M. J. Ganter, C. D. Cress, R. A. DiLeo, and R. P. Raffaelle, *Energy Environ. Sci.* 2, 638 (**2009**).
11. W. Q. Han and A. Zettl, *Nano Lett.* 3, 681 (**2003**).
12. Q. Kuang, S. F. Li, Z. X. Xie, S. C. Lin, X. H. Zhang, S. Y. Xie, R. B. Huang, and L. S. Zheng, *Carbon* 44, 1166 (**2006**).
13. G. D. Du, C. Zhong, P. Zhang, Z. P. Guo, Z. X. Chen, and H. K. Liu, *Electrochim. Acta* 55, 2582 (**2010**).
14. C. Q. Feng, L. Li, Z. P. Guo, and H. Li, *J. Alloys Compd.* 504, 457 (**2010**).
15. C. H. Xu, J. Sun, and L. Gao, *J. Phys. Chem. C* 113, 20509 (**2009**).
16. C. L. Zhu, M. L. Zhang, Y. J. Qiao, P. Gao, and Y. J. Chen, *Mater. Res. Bull.* 45, 437 (**2010**).
17. N. Du, H. Zhang, B. D. Chen, X. Y. Ma, X. H. Huang, J. P. Tu, and D. R. Yang, *Mater. Res. Bull.* 44, 211 (**2009**).
18. M. Dimitrov, T. Tsoncheva, S. F. Shao, and R. Kohn, *Appl. Catal. B-Environ.* 94, 158 (**2010**).
19. S. Zaman, K. Zhang, A. Karim, J. G. Xin, T. Sun, and J. R. Gong, *Diam. Relat. Mat.* 76, 177 (**2017**).
20. H. W. Song, N. Li, H. Cui, and C. X. Wang, *Electrochim. Acta* 120, 46 (**2014**).
21. H. J. Zhang, Z. J. Tan, P. P. Xu, K. Oh, R. F. Wu, W. M. Shi, and Z. Jiao, *J. Nanosci. Nanotechnol.* 11, 11114 (**2011**).
22. Y. Sun, S. R. Wilson, and D. I. Schuster, *J. Am. Chem. Soc.* 123, 5348 (**2001**).
23. N. Wang, J. X. Xu, and L. H. Guan, *Mater. Res. Bull.* 46, 1372 (**2011**).
24. P. Tyagi, A. Sharma, M. Tomar, and V. Gupta, *Sens. Actuator B-Chem.* 248, 980 (**2017**).
25. M. Narjinary, P. Rana, A. Sen, and M. Pal, *Mater. Des.* 115, 158 (**2017**).
26. V. M. Aroutiounian, V. M. Arakelyan, E. A. Khachaturyan, G. E. Shahnazaryan, M. S. Aleksanyan, L. Forro, A. Magrez, K. Hernadi, and Z. Nemeth, *Sens. Actuator B-Chem.* 173, 890 (**2012**).
27. V. M. Aroutiounian, A. Z. Adamyan, E. A. Khachaturyan, Z. N. Adamyan, K. Hernadi, Z. Pallai, Z. Nemeth, L. Forro, A. Magrez, and E. Horvath, *Sens. Actuator B-Chem.* 177, 308 (**2013**).
28. Z. Németh, Z. Pallai, B. Réti, Z. Balogh, O. Berkesi, G. Veréb, A. Dombi, and K. Hernadi, *J. Coat. Sci. Technol.* 1, 137 (**2014**).
29. E. Couteau, K. Hernadi, J. W. Seo, L. Thien-Nga, C. Miko, R. Gaal, and L. Forro, *Chem. Phys. Lett.* 378, 9 (**2003**).
30. G. Kozma, A. Kukovecz, and Z. Konya, *J. Mol. Struct.* 834, 430 (**2007**).
31. Z. Nemeth, B. Reti, Z. Pallai, P. Berki, J. Major, E. Horvath, A. Magrez, L. Forro, and K. Hernadi, *Phys. Status Solidi B-Basic Solid State Phys.* 251, 2360 (**2014**).
32. S. H. Mousavi, H. Haratizadeh, and P. W. de Oliveira, *J. Nanosci. Nanotechnol.* 11, 8233 (**2011**).
33. B. Reti, N. Peter, A. Dombi, and K. Hernadi, *Phys. Status Solidi B-Basic Solid State Phys.* 250, 2549 (**2013**).

Received: 22 September 2017. Accepted: 5 December 2017.